EFFECTS OF PERIMETER RECOMBINATION ON GaAs-BASED SOLAR CELLS

T.B.Stellwag, P.E. Dodd, M.S. Carpenter, M.S. Lundstrom, R.F. Pierret, M.R. Melloch, E. Yablonovitch, and T.J. Gmitter

School of Electrical Engineering
Purdue University
West Lafayette, IN USA 47907

Bell Communications Research
Navesink Research Center
Red Bank, NJ USA 07701-7020

Abstract

Perimeter recombination currents have been experimentally characterized on GaAs p/n heteroface diodes and solar cells with areas ranging from 2.5×10^{-5} to 0.25 cm^2. Under 1-sun operation at the maximum power point, measurements show that the n≈2 perimeter recombination current component degrades the cell's fill factor, but does not greatly effect the open-circuit voltage. The n≈2 perimeter recombination currents are examined theoretically on small area cells using a two-dimensional drift-diffusion device simulator, PUPHS2D. This model verifies the importance and origin of perimeter recombination in heteroface GaAs-based solar cells. Finally, two methods of reducing the n≈2 perimeter recombination are explored.

I. Introduction

Perimeter recombination is commonly neglected in solar cell analysis because it is assumed to be a negligible portion of the dark current in large area cells. However, recent work demonstrates that perimeter recombination dominates the n≈2 dark current in 0.5 cm x 0.5 cm solar cells and is sizeable even in 2 cm x 2 cm cells [1]. Therefore, under 1-sun operation at the maximum power point, the n≈2 current component can degrade the fill factor [2]. Under concentration, the n=1 current typically dominates, so perimeter recombination losses are negligible. However, many solar cell diagnostic measurements are done under low current densities with small area devices. Also, one can envision non-conventional cell designs for which perimeter recombination could even dominate the n=1 current. For these reasons it is important to characterize perimeter recombination, and to learn how to model and minimize these losses.

This paper summarizes a wide range of experimental and theoretical work directed at understanding the physics of perimeter recombination and its consequences for high-efficiency solar cells. The work centers on: (1) characterizing the n≈2 perimeter recombination current in high-efficiency, p-on-n heteroface cells, (2) developing a theoretical understanding of the problem, (3) examining the implications for high-efficiency solar cells, and (4) exploring techniques to minimize perimeter recombination losses.

II. Experimental Characterization of the n≈2 Recombination Current

Device Structure

The structure shown in figure 1 is typically used in high-efficiency solar cell designs to reduce the n=1 diffusion current component due to the large surface recombination velocity of GaAs. The design surrounds the GaAs p^+/n junction with an epitaxial layer of the wider-bandgap lattice-matched material $Al_xGa_{1-x}As$. This wide-bandgap material allows light to penetrate into the GaAs region without being absorbed. Also, because the materials are lattice-matched there are few interfacial states at the heteroface junction. The reduction of states greatly reduces the recombination velocity at the front and back surface, thereby suppressing the n=1 diffusion current component. Since the n=1 component is suppressed, the n≈2 perimeter recombination current is the largest contributor to the dark current at biases of about one volt or less.

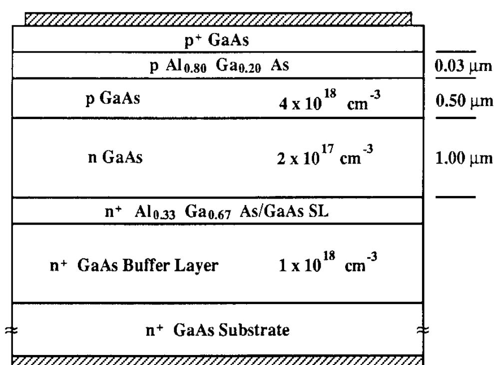

Fig. 1. Cross-section of MBE-grown diodes.

Film Growth and Device Processing

The GaAs and $Al_xGa_{1-x}As$ layers were grown on a two-inch liquid-encapsulated-Czochralski (LEC) (100)-GaAs substrate in a Varian GEN II molecular beam epitaxy (MBE)

0160-8371/90/0000-0442 © $1.00 1990 IEEE

system at Purdue University. The source materials consisted of elemental gallium, arsenic, and aluminum, with beryllium and silicon used as p- and n-type dopants, respectively. The layers were grown at a substrate temperature of 600°C (the oxide desorption temperature was 580°C). A superlattice (SL) layer consisting of 20 periods of 28 angstrom $Al_{0.33}Ga_{0.67}As$ barriers and 31 angstrom GaAs wells was incorporated in the film structure to reduce diffusion of impurities from the substrate into the growing film [3]. Reflection high-energy electron diffraction patterns were used to monitor the growth rate and growth conditions. Each of two gallium furnaces produced a flux corresponding to a growth rate of 0.5 µm/hr, for a net growth rate of 1.0 µm/hr. The As_4 to total Ga beam equivalent pressure measured with an ion-guage in the substrate growth position was 27.

In order to separate the current components, the processed devices consisted of squares with areas ranging from 2.5×10^{-5} to 0.01 cm^2 and perimeter-to-area (P/A) ratios varying from 40 to 800 cm^{-1}. The masking levels also included devices necessary to study the effect of crystallographic orientation on perimeter recombination [4], and 0.5 cm x 0.5 cm solar cells. The processing was as follows. First, a back ohmic contact was formed by alloying indium at 350°C for 1 minute because a nonindium wafer mount was used during the MBE growth. Front metallization lift-off patterns were then defined, Ti/Au was electron-beam evaporated to form non-alloyed ohmic contacts, and the photoresist was dissolved in acetone to remove the excess metal. Following the metal deposition, mesas were defined using conventional photolithography and etched in a 25°C methanol:H_2O_2:H_2O:H_3PO_4 3:1:1:1 solution for 1 min 15 sec. The etch rate was approximately two microns per minute making this etch suitable for mesa isolation.

Device Characterization

The forward-biased dark current versus voltage characteristics of the p^+/n heteroface diodes were measured using an HP 4145 semiconductor parameter analyzer. Figure 2 shows the measured current and ideality factor (n-factor) of a typical cell as a function of applied bias. At low biases, these diodes have constant n-factors of 1.9 which indicate that in this range their dark current is dominated by recombination in a space-charge region. For ease of presentation, this current will be referred to as an n≈2 recombination current. At higher biases, the n-factor approaches 1.5 before the effects of series resistance become appreciable, suggesting that another mechanism is responsible for the decrease. The remainder of the device characterization develops the experimental method used to extract the dominant current components as a function of applied voltage.

The saturation current densities of the n=1 diffusion current (J_{o1}) and the n≈2 recombination current (J_{o2}), and the ideality factor appear in the expression for diode current.

$$J = J_{o1}(e^{qV/kT} - 1) + J_{o2}(e^{qV/2kT} - 1) \qquad (1)$$

These unknowns can be determined from the experimental data

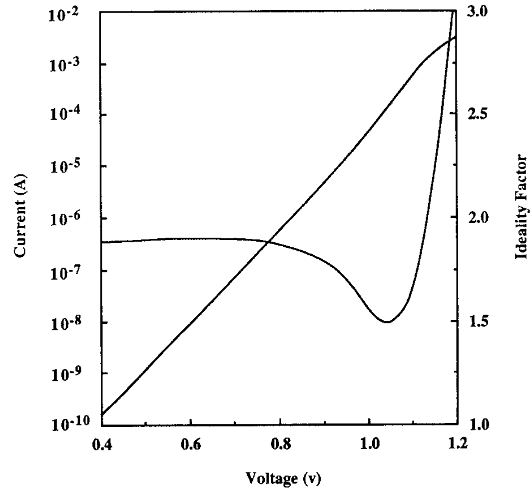

Fig. 2. Typical dark current and diode ideality factor as a function of voltage.

by the method of least squares applied to the diode current versus voltage characteristics. The values of n, J_{o1}, and J_{o2} were extracted for the diodes with P/A ratios between 40 and 800 cm^{-1}. These values are plotted in figure 3 as a function of P/A ratio. While the n=1 diffusion saturation current densities (J_{o1}) remained constant with increasing P/A ratio, the n≈2 recombination saturation current densities (J_{o2}) increased linearly with P/A ratio.

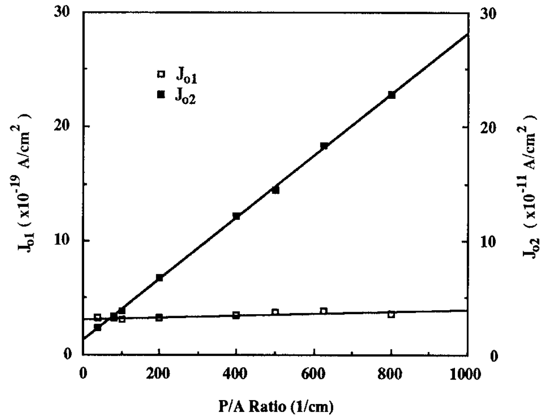

Fig. 3. J_{o2} versus P/A Ratio at 25°C.

The saturation current densities, J_{o1} and J_{o2}, can be written as

$$J_{on} = J_{onB} + J'_{onP}(P/A) \qquad (n=1,2) \qquad (2)$$

where J_{onB} (A/cm^2) is the bulk saturation current density, J'_{onP} (A/cm) is the perimeter saturation current density, P (cm) is the perimeter of the device, and A (cm^2) is the area of the device. Figure 3 along with equation 2 suggest that for the n=1 diffusion current, the perimeter component is negligible when compared to

the bulk component for any size of device. In contrast, the perimeter component of the n≈2 recombination current is dominant for small devices and is a significant portion of the current for devices as large as 0.25 cm^2. From the intercept of the J_{02} versus P/A ratio plot, the 25°C bulk saturation current density, J_{02B}, is $1.31x10^{-11}$ A/cm^2. The value of J'_{02P} extracted from the slope of the same plot is $2.69x10^{-13}$ A/cm. This value for J'_{02P} represents a factor of four improvement over those reported previously [1,5,6]. Diagnostics on record efficiency solar cells which were mesa-isolated with the same phosphoric/peroxide based etchant used in this work yielded similar results [7]. This decrease in J'_{02P} could be partially responsible for recent efficiency increases in GaAs solar cells.

Following Henry *et al.* [8], the perimeter recombination coefficient, J'_{02P}, can be written as,

$$J'_{onP} = qn_iS_oL_s \quad (3)$$

where n_i is the intrinsic carrier concentration, S_o is the surface recombination velocity, and L_s is an effective surface diffusion length. The measured S_oL_s product at 25°C for these devices is 0.94 .

Further analysis of the experimental data was necessary to determine the validity of the results obtained from the J_{on} versus P/A ratio plot. In equations 1 and 2 it was assumed the the n-factor of the bulk region equaled that of the exposed surface. A more accurate expression would involve separate ideality factors for the bulk and the perimeter. If n_B represents the bulk n-factor, and n_P represents the perimeter n-factor, equation 1 can be rewritten as,

$$J = J_{onB}\left(e^{qV/n_BkT} - 1\right) + J'_{onP}\left(e^{qV/n_PkT} - 1\right)(P/A) \quad (4)$$

where J_{onB} and J'_{onP} now include the n=1 and n≈2 current components. The procedure used to separate the bulk and perimeter current components as a function of bias is described in a recent publication [9]. The results, shown in figure 4, confirm that the ideality factors of the bulk and the surface differ throughout the indicated bias range.

For biases below 0.8 volts, the calculated value of the n-factor of the perimeter closely parallels that of the diode n-factor, whereas the n-factor of the bulk is significantly lower. This again suggests that the primary current mechanism at low biases is the n≈2 perimeter recombination current. Previously, it was assumed that n_B=n_P=n in order to extract values for the n≈2 bulk and perimeter saturation current densities. The assumption that the ideality factor of the surface equals that of an actual diode is reasonable, but the assumption that n_B=n introduces error into the extraction of J_{02B}. Therefore, the intercept of the J_{02} versus P/A ratio plot only describes the upper limit of the bulk saturation current density.

Though there is a slightly negative slope to the perimeter ideality factor at high biases, it is insignificant in comparison with the decrease in the bulk ideality factor. This again emphasizes that the n=1 current component is primarily due to recombination in the quasi-neutral bulk region of the diode. These experimental results were corroborated with a two-dimensional device simulator, PUPHS2D, described in the next section.

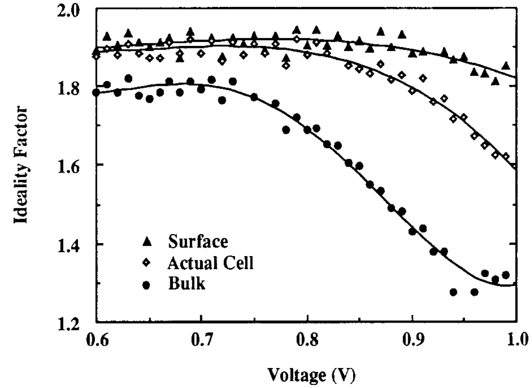

Fig. 4. Ideality factor versus bias for the surface, the bulk, and an actual cell.

III. Theoretical Characterization of the n≈2 Recombination Current

A two-dimensional drift-diffusion device simulator, PUPHS2D [10], was used to model the experimental devices in order to verify the importance and origin of perimeter recombination in heteroface GaAs solar cells. The model was expanded to treat surface recombination through Shockley-Read-Hall (SRH) recombination via deep level traps, and includes Fermi level pinning. The exact formulation of the surface model is discussed elsewhere [9]. The perimeter model parameters used for all simulations were surface recombination velocities of $2x10^5$ cm/s and a total surface trap density of 10^{13} cm^{-2}. Equal concentrations of acceptor-like and donor-like surface traps located at midgap were assumed.

The simulated and experimental current-voltage characteristics and ideality factor versus bias agree well. Figure 5 shows the simulated bulk and perimeter components of the diode current. For this diode, which has a P/A ratio of 625 cm^{-1}, the perimeter current is dominant for all biases less than one volt.

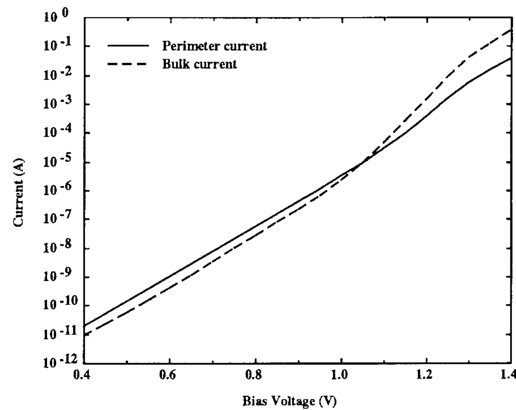

Fig. 5. Simulated bulk and perimeter current components in GaAs heteroface diode as a function of bias.

Careful examination of figure 5 reveals that both the bulk and perimeter current ideality factors drop from n≈2 at high bias. For the bulk current, this is due to recombination of injected carriers in the neutral base and emitter. The drop in perimeter current ideality factor at high bias has been previously reported [11] and will be studied in detail elsewhere [9].

The origin of n≈2 recombination current is clarified with the help of figure 6, which shows the internal volume recombination rate within the diode at a bias of 0.6 V. The bulk recombination peak within the junction space-charge region is clearly visible. It should be noted, however, that the recombination rate is plotted on a logarithmic scale and the recombination shown at the perimeter far outweighs the bulk contribution at this bias. It is seen that the perimeter recombination is also greatest in the vicinity of the junction space-charge region. This is more clearly seen in figure 7, which displays the normalized perimeter recombination rate for a variety of bias conditions. The perimeter recombination rate is highly peaked in the junction space-charge region for moderate bias, which leads to n≈2 perimeter current. As the bias is increased, the surface depletion layer induced by the charged surface traps begins to fill with injected carriers, altering the recombination profile and lowering the perimeter current ideality factor.

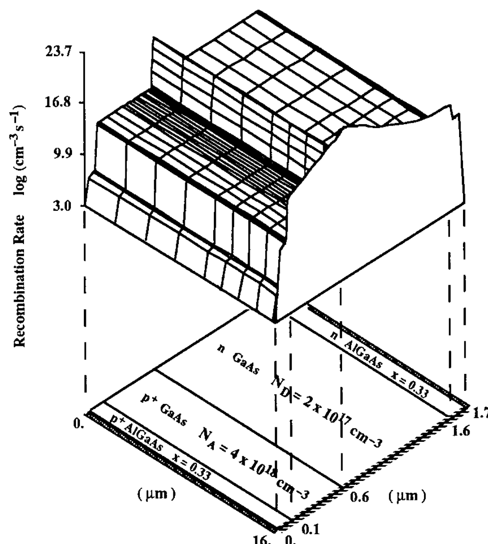

Fig. 6. Internal volume recombination rate in GaAs heteroface diode with surface states under 0.6 V of forward bias. Viewed on logarithmic scale.

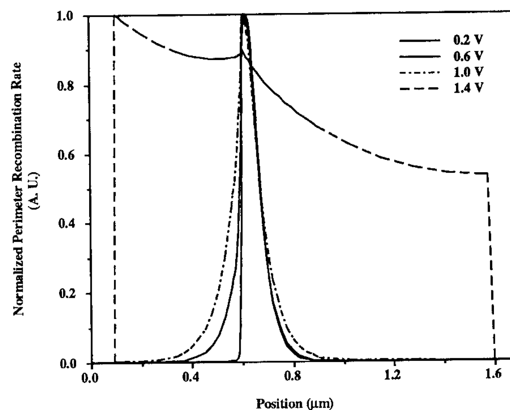

Fig. 7. Perimeter recombination profiles for various bias voltges. Note sharp peak in junction space-charge region under moderate bias.

IV. Implications for High-Efficiency Solar Cells

As previously described, the n≈2 perimeter recombination current component is a significant portion of the forward-biased dark current of 0.5 cm x 0.5 cm MBE-grown GaAs solar cells. A comparison between high-efficiency MBE-grown and MOCVD-grown GaAs solar cells reveals that the n≈2 bulk saturation current density is six times less in the MOCVD-grown cells, while the n≈2 perimeter recombination components are comparable [7]. Hence, the effect of n≈2 perimeter recombination current on high-efficiency GaAs solar cell performance is more readily examined using the parameters of the MOCVD-grown device.

Using the values of J_{02B} obtained from the 24.8% efficient MOCVD-grown solar cells, the perimeter current component accounts for fourteen percent of the n≈2 perimeter dark current at V_{OC}, and for over 53 percent of the n≈2 perimeter dark current at V_{MP}. Under 1-sun operation at the maximum power point, the n≈2 perimeter recombination current degrades the fill factor but does not greatly effect V_{OC}. Using a value of J'_{02P} corresponding to a freshly prepared surface, the calculated fill factor is 0.871 for J_{SC}=27.67 mA/cm^2. If the n≈2 perimeter current component is removed from the calculation, the fill factor becomes 0.883 and the efficiency of the cell increases by 0.5%. The calculated light-current versus voltage characteristics with and without the n≈2 perimeter recombination current component are shown in figure 8.

It is noted in several publications that the n≈2 current component degrades with time and photon exposure [7,12]. Tobin *et al.* measure a 30% increase in J_{02P} over a period of thirty days. Included in figure 8 is the light-current versus voltage plot of the cell exhibiting this increase in perimeter current. This plot indicates that the increase in J_{02P} results in a slight decrease in the device current (output power). Since the short-circuit current and open-circuit voltage do not change, the fill factor also decreases slightly. Others have shown that photon exposure causes a larger reduction of the device current but does not significantly change V_{OC} [12]. This effect could also be attributed to perimeter degradation. For these reasons, it would be important to develop a treatment which would reduce the effect of perimeter aging.

Perhaps the most important implication of n≈2 perimeter recombination current is its effect on small-area test structures. Since perimeter recombination dominates the current of small-area devices, it must be accounted for in solar cell analysis and design .

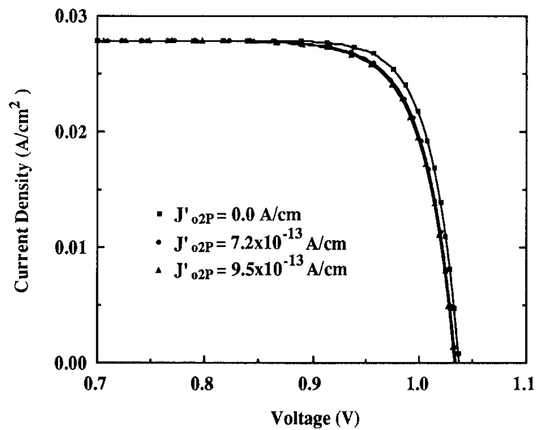

Fig. 8. Calculated light-current versus voltage characteristics with and without the n≈2 perimeter recombination current.

V. Methods of Reducing Perimeter Recombination

Surface Treatments

A temporary reduction in perimeter currents in GaAs p/n junctions can be obtained using Na_2S or $(NH_4)_2S$ chemical passivation treatments [13]. A chemical treatment which coats the mesa edges of GaAs p/n junctions with As_2S_3 glass and results in a permanent reduction in perimeter currents was recently developed at BELLCORE [14]. The current-voltage characteristics of a typical device of area $2.5x10^{-5}$ cm^2 before and after the As_2S_3 chemical treatment are shown in figure 9. These results show nearly an order of magnitude reduction in current following the As_2S_3 treatment.

Orientation Dependence of Perimeter Recombination

Perimeter recombination can be minimized by properly orienting the mesa with respect to the crystallographic axes. Figure 10 shows the n≈2 perimeter recombination current for an edge as a function of orientation. This value of perimeter saturation current density, J'_{o2P}, varies by more than a factor of five as the device is rotated from 0 to 90 degrees (where 0 degrees is defined as the <011>-direction). The experimental method used to measure this orientation dependence is described in detail in a recent publication [4]. These results suggest that with proper device design, perimeter recombination currents could be substantially reduced thereby enhancing 1-sun GaAs cell performance.

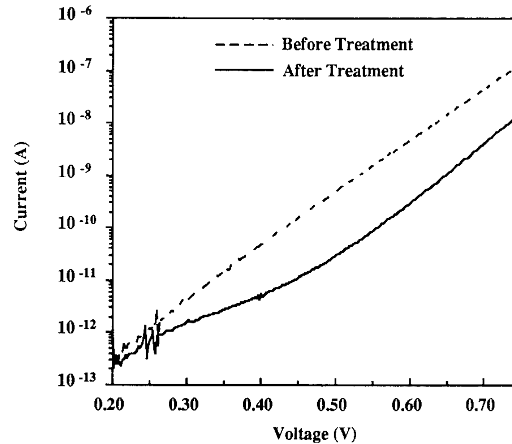

Fig. 9. Current-Voltage characteristics of a typical device of area $2.5x10^{-5}$ cm^2 before and after the As_2S_3 chemical treatment.

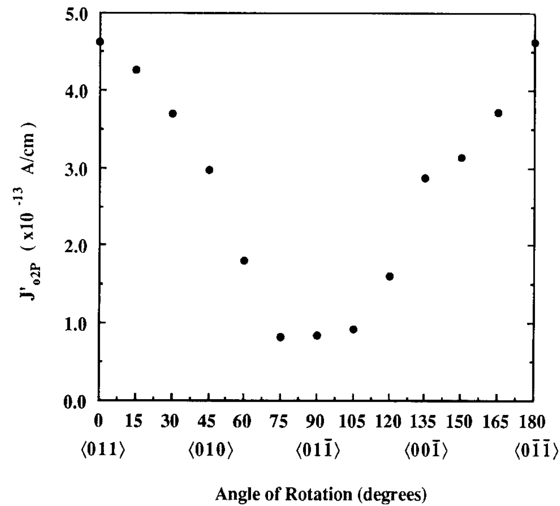

Fig. 10. The n≈2 perimeter recombination current for an edge as a function of device orientation.

VI. Conclusions

The results of this work demonstrate that perimeter recombination has important consequences in high-efficiency GaAs-based solar cells. Perhaps more important is the fact that this effect dominates the small area diagnostic devices often used in cell development. This work provides the theoretical and experimental characterization needed to model such effects in modern GaAs solar cells.

Acknowledgement

This work was supported by the Solar Energy Research Institute for the U.S. Department of Energy under subcontract XL-5005018-1.

References

[1] P.D. DeMoulin, S.P. Tobin, M.S. Lundstrom, M.S. Carpenter, and M.R. Melloch, *IEEE Elect. Dev. Lett.*, vol. 9, p.368, 1988.

[2] S.P. Tobin, et al., *Solar Cells*, vol. 24, p. 103, 1988.

[3] K.L Tan, M.S. Lundstrom, and M.R. Melloch, *Appl. Phys. Lett.*, vol. 48, p. 428, 1986.

[4] T.B. Stellwag, M.R. Melloch, M.S. Lundstrom, M.S. Carpenter, and R.F. Pierret, *Appl. Phys. Lett.*, vol., p., 1990.

[5] C.H. Henry, R.A. Logan, and R.R. Merrit, *Appl. Phys. Lett.*, vol. 31, p.454, 1977.

[6] T.J. deLyon, H.C. Casey Jr., M.L. Timmons, J.A. Hutch, and D.H. Dietrich, *Appl.Phys. Lett.*, vol. 50, p. 1903, 1987.

[7] S.P. Tobin, S.M. Vernon, C. Bajgar, S.J. Wojtczuk, M.R. Melloch, A. Keshavarzi, T.B. Stellwag, S. Venkatesan, M.S. Lundstrom, and K.A. Emery, *IEEE Trans. on Elec. Dev.*, vol. 37, p. 469, 1990.

[8] C.H. Henry, R.A. Logan, and F.R. Merritt, *J. Vac. Sci. Technol.*, vol. 15, p. 1471, 1978.

[9] P.E. Dodd, T.B. Stellwag, M.S. Lundstrom, and M.R. Melloch, To be published *IEEE Trans. on Elec. Dev.*

[10] P.D. DeMoulin and M.S. Lundstrom, *IEEE Trans. Elect. Dev.*, vol. 36, p. 897, 1989.

[11] S. Tiwari, *J. Appl. Phys.*, vol. 64, p. 5009, 1988.

[12] B. Anspaugh and R. Kachare, *Conf. Rec. 20th IEEE Photovoltaic Spec. Conf.*, p. 985, 1988.

[13] M.S. Carpenter, et al., *Appl. Phys. Lett.*, vol. 52, p. 2157, 1988.

[14] E. Yablonovitch, et al., To be published.